Control Engineering Practice 25 (2014) 66–74

Contents lists available at ScienceDirect

Control Engineering Practice

journal homepage: www.elsevier.com/locate/conengprac

Linear algebra based controller design applied to a bench-scale oenological alcoholic fermentation

Gustavo Scaglia [a,*], Pablo M. Aballay [a], M. Emanuel Serrano [a], Oscar A. Ortiz [a], Mario Jordan [c], Martha D. Vallejo [b]

[a] Instituto de Ingeniería Química, Universidad Nacional de San Juan, Av. Libertador San Martín Oeste 1109, San Juan J5400ARL, Argentina
[b] Instituto de Biotecnología, Universidad Nacional de San Juan, Av. Libertador San Martín Oeste 1109, San Juan J5400ARL, Argentina
[c] Dto. de Ing. Eléctrica y de Computadoras UNS- Instituto Argentino de Oceanografía (IADO-CONICET)- edificio E 4, km 7, Camino La Carrindanga, Bahía Blanca, Argentina

ARTICLE INFO

Article history:
Received 20 November 2012
Accepted 3 January 2014

Keywords:
Tracking control
Difference equations
Non-isothermal operation
Oenological alcoholic fermentation
Yeasts growth

ABSTRACT

This work presents a controller design for a non-isothermal alcoholic fermentation to produce wines in a bench-scale bioreactor. The main controller objective is that the system tracks an optimal operation trajectory to produce wines with constant quality. This trajectory is previously determined for the biomass and for the CO_2 produced by the fermentation. To meet the goal, the process is approximated using numerical methods, and then, the problem is posed like solving a system of linear equations. The necessary conditions for the system of linear equations has exact solution are analyzed. Afterwards the control action is obtained by solving the system of linear equations. The methodology success is shown using experimental results.

1. Introduction

A bioprocess is a method or operation of preparing a biological material, especially a product of genetic engineering, for commercial use. Generally include one or more bioreactors, also named fermenters in the wine industry. Because of complex nature of microorganism growth and product formation in batch and fed-batch cultures, which are often employed in preference to continuous cultures, the control of bioprocesses continues to be a challenge to chemical engineers (Komives & Parker, 2003).

During fermentation, the microbial or enzymatic agents are grown in a controlled mode and the feedstock is converted or transformed through biochemical reactions (Valencia Peroni, 2003). From the point of view of cell growth as a result of the utilization of nutrients, microbial biomass increases over time.

One of the main problems in non-linear control systems is the trajectory tracking. In general, the objective is to compute the control actions so that the system tracks a previously established trajectory. Li and Wozny (2001) considered the trajectory tracking problem for multiple-fraction batch distillation. Since the latter system is non-linear and time dependent, the objective cannot be achieved with a conventional proportional integral derivative (PID) controller, the use of more advanced controllers is necessary. Golshan, MacGregor, Bruwer, and Mhaskar (2010) considered an alternative model predictive control for trajectory tracking based on latent variable models; such algorithms were applied to a batch reactor with an exothermic reaction. Moreover, controllers based on neural networks have been used in trajectory tracking problems (Horn, 2001; Sjoberg & Agarwal, 2002). Horn (2001), used input–output linearization via states feedback and applied that technique for trajectory tracking on a batch polymerization reactor. Sjoberg and Agarwal (2002) applied the same strategy on an exothermic batch reactor, as well. Tebbani, Dumur, and Hafidi (2008), determined first, the optimal trajectory of a fed-batch bioreactor, and the optimal trajectory tracking was then performed thanks to cascaded control architecture. This latter has an inner loop consisting of a linearizing state-feedback control law, and an outer one including a proportional integral (P.I.) controller, in order to cancel steady tracking errors. Cédric, Michel, Lionel, Brigitte, and Chabriat (2011) presents an observer coupled to a multivariable set-point tracking control, based on an input–output linearization algorithm.

Main operation variables in fermentations are: pH, temperature, dissolved oxygen concentration, agitation speed, foam level, and others (Morari & Zafiriou, 1997). For example, temperature is seen as a fine tool for better regulation of the fermentation progress, in accordance with a winemaking strategy depending on the desired wine (Torija et al., 2003; Molina, Swiegers, Varela, Pretorius, & Agosin, 2007; Romero Cascales, 2008). With on-line monitoring of the fermentation rate, winemaking operations

* Corresponding author. Tel.: +54 264 4238148.
E-mail addresses: gscaglia@unsj.edu.ar, gustavoscaglia@yahoo.com.ar (G. Scaglia).

0967-0661/$ - see front matter © 2014 Elsevier Ltd. All rights reserved.
http://dx.doi.org/10.1016/j.conengprac.2014.01.002

(temperature regulation, nutrient additions, pumping, etc.) can be adapted to actual fermentation behavior. Some studies suggest that controlling the fermentation rate may be at least as important as controlling the temperature; one of them highlights the benefits of controlling CO_2 production rate (Sablayrolles, 2009). Additionally, fermentation presents important interactions between cell bio-kinetics and the bioreactor hydrodynamic conditions, which lead to models with non-linear and unsteady characteristics. Therefore, advanced optimization and control tools for monitoring and controlling strictly the process, are required. The implementation of advanced control strategies needs appropriate dynamic models and reliable on-line measurements (Henson, 2003). Furthermore, alcoholic fermentation models can assure wine quality and reproducibility among batches (Zenteno, Pérez-Correa, Gelmi, & Agosin, 2010), as well. Moreover, non-isothermal models developed from laboratory or bench-scale alcoholic fermentations have been validated or tested with good performance, or highlighted their possible scaling-up to industrial tanks (Phisalaphong, Srirattana, & Tanthapanichakoon, 2006; Colombié, Malherbe, & Sablayrolles, 2007; Malherbe, Fromion, Hilgert, & Sablayrolles, 2004; Coleman, Fish, & Block, 2007). Casalta et al. (2010) have carried out a comparison of laboratory and pilot-scale fermentations in winemaking conditions by means of the study of kinetics and the production of aromatic compounds of own and other authors′ experiments as the latter mentioned. Authors′ contributions on modeling and advanced controlling of oenological alcoholic fermentations are: an advanced temperature control system based on an improved non-isothermal phenomenological model that allows tracking complex temperature profiles to achieve optimal quality of wine (Ortiz, Vallejo, Scaglia, Mengual, & Aballay, 2009), and the design of a controller based on numerical methods applied to a bench-scale bioprocess for good-quality wines (Scaglia, Rosales, Quintero, Mut, & Agarwal, 2010b).

From a mathematical point of view, models must be at the same time accurate and simple to be used in on-line control algorithms. In previous contributions, the authors have addressed isothermal and non-isothermal first principles and hybrid neural models, and an improved isothermal phenomenological model with satisfactory capability to approximate the main variables profiles of oenological alcoholic fermentations (Vallejo et al., 2005; Ortiz, Aballay, & Vallejo, 2006; Aballay, Scaglia, Vallejo, & Ortiz, 2008; Scaglia, Quintero, Mut, & di Sciascio, 2009b). Also, the improved phenomenological model has been extended to a non-isothermal operation (Aballay, Scaglia, Vallejo, Rodríguez, & Ortiz, 2010).

The oenological alcoholic fermentation control is carried out, mostly, by means of temperature manipulation, thus, cells population and main fermentation variables are regulated. The desired organoleptic wine properties can be obtained in this fashion, which depend on population of the proper selected yeast as well as its variation in time. Cells as living beings evolve as such and have precise needs of nutrition and the medium they live into. Yeasts are sensitive to temperature, and concentrations of oxygen, sugars, minerals and nitrogen-based substances. It is usual that by using the same varietal must (grape juice) and composition, pure yeast starter culture, initial conditions and constant temperature to carry out an oenological alcoholic fermentation, the cells population evolution in time has not the same performance among batches, which affects the final wine quality (Pretorius, 2000; Torija et al., 2003). This is the reason why fermentation reproducibility among batches is a current trouble.

In this work, an advanced trajectory tracking control for an oenological alcoholic fermentation operated on batch mode is presented. The complex dynamics, nonlinearity and non-stationary of fermentation make the control of this bioprocess, is a difficult task. Thus, the main control objective was that the key process variables evolve in time tracking an optimal trajectory previously defined. More specifically, the given trajectories were the main process state variables, as viable cells concentration and CO_2 released, from which a suitable temperature profile for desire fermentation evolution was determined to assure fermentation reproducibility and the wine quality. This simple approach suggests that knowing the desired state value, a value for the required control action can be found; that force the system to move from its current state to the desired one. The developed controller for tracking the optimal trajectory in some states was based on determining the desired trajectories of the other state variables. Such states were determined by analyzing the necessary conditions so that the linear equations system had exact solution. Then, the control signals were obtained by solving the system of linear equations. Furthermore, variables transformations in the controller design were not necessary either. This technique for controllers design for trajectory tracking has been applied to non-linear multivariable systems as shown in Scaglia, Aballay, Vallejo, Suarez, and Ortiz (2010a), Scaglia, Aballay, Mengual, Vallejo, and Ortiz (2009a), Rosales, Scaglia, Mut, and di Sciascio (2009), and a complex system consisting of a set of nonlinear multivariable systems that must work in a cooperative manner (Rosales, Scaglia, Mut, and di Sciascio, 2011).

The work is organized as follows. Section 2 presents a brief description of fermentation in winemaking and its modeling. Also, the used non-isothermal model with considerations on its components and parameters, as well as, on main properties, is described in this section. In Section 3, details about the controller design are depicted. Experimental results showing the accomplishment of the proposed controller are illustrated in Section 4. Finally, Section 5 presents the discussion regarding major obtained results, and analyzes the contribution of the work and outlines some topics to be addressed in future works.

2. Process model

The reductive metabolic pathway characterizes the yeast population growth in anaerobic conditions. This behavior can be represented as:

$$S \underset{\rightarrow}{\text{yields}} \; Y_{X/S}X + Y_{CO_2/S}CO_2 + Y_{Eth/S}Eth$$

In this equation, X, S, CO_2 and Eth correspond to viable cells, carbon source (glucose and fructose), carbon dioxide and ethanol concentrations (kg m^{-3}), respectively. Whereas, $y_{x/s}$, $y_{CO_2/s}$ and $y_{Eth/s}$ are stoichiometric coefficients. In Eq. (1), only the most abundant products are stated. During grape must fermentation, a number of other minor, but important metabolites are produced (glycerol, higher alcohols, esters, etc.). These by-products are related with sensory attributes of wine. According to Coleman et al. (2007), model′s prediction capabilities of sugar and ethanol are important from an enologist′s point of view, due to they are the most important state variables.

Remark 1. In this paper the concept of cells, biomass and yeast are used in an equivalent way.

The ethanol production reaction from glucose is the following:

$$C_6H_{12}O_6 \rightarrow 2CH_3CH_2OH + 2CO_2 \tag{1}$$

Metabolite accumulation in the extra-cellular medium has been modelled by a set of ordinary differential equations (ODE) based on the mass balances on cells, substrate as carbon source and ethanol. Released carbon dioxide is also included in the model because such variable provides an inexpensive and convenient way to monitor the evolution of the other process variables, especially those stoichiometrically related. Model assumptions were: balance parameters of the model, including pH, were stated constant. Fermentation was not nitrogen source-limited; this is viable, based on information about the chemical composition of the local musts. In the energy balance, Eq. (8): heat losses due to CO_2 evolution, water evaporation and ethanol and flavour losses were neglected; the average grape juice-wine density and specific heat, and all physical properties were uniform in the fermenting mass bulk. They were considered constant with the (bioreactor) temperature T [K] and time [h]. Convective heat transfer coefficient of fermentation mass, implicitly included in Eq. (8), was constant (Colombié et al., 2007). In the cooling jacket: water properties variations and the fouling factor in jacket side were neglected. Heat transfers by radiation and conduction were considered negligible as well.

The following equations describe the time course of X, S, Eth and CO_2 according to the mass balances on:
Viable cells:

$$\frac{dX}{dt}=\underbrace{\frac{e^{-(CO_2-CO_{2,\,95})}}{e^{(CO_2-CO_{2,\,95})}+e^{-(CO_2-CO_{2,\,95})}}A\,\mu_m\frac{S}{S+Ks\,B^a}X\left(1-\frac{X}{A\,\mu_m\frac{S}{(S+Ks\,B^a)\beta}}\right)}_{\text{yeastgrowth}}+$$

$$+\underbrace{\left[1-\frac{e^{-(CO_2-CO_{2,\,95})}}{e^{(CO_2-CO_{2,\,95})}+e^{-(CO_2-CO_{2,\,95})}}\right]\left(C\,X\frac{dS}{dt}-D\,X\right)}_{\text{deathgrowth}} \tag{2}$$

Substrate:

$$\frac{dS}{dt}=\frac{1}{Y_{X/S}}\left[-X\left(\mu_m\frac{S}{S+Ks\,B^b}-E\,X\right)\right]-\mathrm{F}\,\mathrm{X} \tag{3}$$

Carbon dioxide:

$$\frac{dCO_2}{dt}=G\mu_m\frac{S}{S+Ks\,B^c}X+\frac{d}{d\,t}\left(H\,\mu_m\frac{S^2}{\left(S+Ks\,B^d\right)\left(S+Ks\,B^e\right)}X+I\,X\right) \tag{4}$$

Ethanol:

$$\frac{dEth}{dt}=\frac{1}{Y_{CO_2/Eth}}\frac{dCO_2}{dt} \tag{5}$$

The previous mass balances and the energy balance in the reactor and its cooling jacket constitute the non-isothermal kinetic model. The effect of fermentation temperature on the maximum specific cellular growth and death rates, μ_m and D, in [h^{-1}], respectively, have the Arrhenius's form in Eq. (6), and the form used by Valencia Peroni, 2003, in Eq. (7),

$$\mu_m(T)=\gamma\times\frac{T\times e^{-\frac{Ea}{R\times T}}}{1+e^{-\frac{\Delta G_d}{R\times T}}} \tag{6}$$

$$D(T)=\begin{cases} if\ \ T\geq 303\ \ K\rightarrow D=\frac{(T-303)}{f}+D_0 \\ Otherwise\rightarrow D=D_0\end{cases} \tag{7}$$

γ is the maximum cellular growth rate per Kelvin degree [h^{-1} K^{-1}], Ea is the activation energy [kJ kmol^{-1}] and ΔGd [kJ kmol^{-1}] is Gibbs free energy change of the fermentation reaction, D_0 is the specific cellular death constant [h^{-1}] when temperature is 303 K, and f is a coefficient [h K] related to D_0 at a temperature higher than 303 K. The before mentioned parameters were adjusted by the least-square method, using experimental data obtained from the cultures described on the experimental setup (Item 4. R is general gas constant [kJ kmol^{-1} K^{-1}]. The initial values for μ_m and D are 0.109 and 0.0081 h^{-1}, respectively.

The balance for the energy accumulation in the bioreactor is,

$$\frac{d(\rho_r\times V_r\times Cp_r\times T)}{dt}=Y_{H/CO_2}\times V_r\times\frac{dCO_2}{dt}-Q \tag{8}$$

V_r [m^3] is the volume. Y_{H/CO_2}[W h produced kg^{-1} CO_2 released] is the energy due to the carbon dioxide released by the bio-reaction. It was obtained by stoichiometry (Eq. (1)) from $Y_{H/S}$, the likely energetic yield on substrate consumed. Q [W] represents the exchanged heat between the fermenting mass and the cooling jacket (see details in Aballay et al., 2008). ρ_r [kg m^{-3}] and C_{pr} [W h kg^{-1} K^{-1}] are density and specific heat of the fermenting mass.

Numerical values of preceding model parameters [Eqs. (2)–(8)] and their description are shown in Table A1, Appendix A (Scaglia, Quintero, Mut, & di Sciascio, 2009; Aballay et al., 2010).

Then, the aim of this work is to find the values of μ_m, D and after that T, so that the bioreactor can follow a pre-established trajectory. $Xref(t)$, CO_2 $ref(t)$ and $Sref(t)$ are variables that composed the reference trajectory; these variables are also solution of the differential Eqs. (2) and (4) and correspond to successful experimental test performed in our laboratories.

3. Controller design

First, $\mu_m(T)$ was computed in the cellular growth phase, then μ_m and D were computed in the cellular death phase. Subsequently, temperature was determined by using Eqs. (6) and (7), so that X and CO_2 follow the previously-established optimum profile.

3.1. Cellular growth

In the cellular growth phase, the term $\text{cellular}_{\text{growth}}=e^{-(CO_2-CO_{2,\,95})}/(e^{(CO_2-CO_{2,\,95})}+e^{-(CO_2-CO_{2,\,95})})$ is approximately equal to 1. The time variation of the aforementioned term is included in Fig. 2(a), where it takes the value 0 (zero) rapidly, during the cellular death phase as can be seen. Additionally, the transition region is negligible if it is compared to the total reaction time. Then, the evolution of the cells concentration at this phase was determined by,

$$\frac{dX}{dt}=A\,\mu_m\frac{S}{S+Ks\,B^a}X\left(1-\frac{X}{A\,\mu_m\frac{S}{(S+Ks\,B^a)\beta}}\right) \tag{9}$$

Considering the following differential equation:

$$y'=f(y,t)\quad y(0)=y_0$$

where the aim is to know the value of $y(t)$ at discrete time instants $t=nT_0$, where T_0 is the sampling period and $n\in\{0,1,2,3.....\}$, the value for variable $y(t)$ at $t=nT_0$ will be denoted as $y(n)$. If, for example, one wishes to compute the value for $y(n+1)$ by knowing the value $y(n)$, one should integrate Eq. (1) over the time interval $nT_0\leq t\leq(n+1)T_0$, then,

$$y(n+1)=y(n)+\int_{nT_0}^{(n+1)T_0}f(y,t)dt$$

There are several numerical integration methods, with their corresponding algorithms to calculate the value of $y(n+1)$. For instance, an approach could be through equations.

$$y(n+1)\cong y(n)+T_0f(y(n),t(n))$$

$$y(n+1)\cong y(n)+T_0f(y(n+1),t(n+1))$$

In numerical methods, these approximations are called the explicit and implicit Euler methods, respectively.

Values of $X(t),S(t),CO_2(t)$ at the discrete time $t=nT_0$, where T_0 is the sampling period and $n\in\{0,1,2,3,\cdots\}$, will be denoted as $X(n),S(n)$ and $CO_2(n)$, respectively. If the implicit Euler`s approximation (Stoer & Bulirsch, 1992) is used, then Eqs. (3), (4) and (9) can be represented by,

$$X(n)=X(n-1)+T_0 A\,\mu_m(n)\frac{S(n)X(n)}{S(n)+Ks\,B^a}\left(1-\frac{X(n)}{A\,\mu_m(n)\frac{S(n)}{(S(n)+Ks\,B^a)\beta}}\right) \tag{10}$$

$$S(n)=S(n-1)+\frac{T_0}{Y_{X/S}}\left\{\left[-X(n)\left(\mu_m(n)\frac{S(n)}{S(n)+Ks\,B^b}-E\,X(n)\right)\right]-F\,X(n)\right\} \tag{11}$$

$$CO_2(n)=CO_2(n-1)+T_0\Big\{G\mu_m(n)\tfrac{S(n)}{S(n)+Ks\,B^c}X(n)+\cdots$$
$$\cdots\quad+\frac{1}{T_0}[(H\,\mu_m(n)\frac{S(n)^2}{(S(n)+Ks\,B^d)(S(n)+Ks\,B^e)}X(n)+I\,X(n))-\quad\cdots$$
$$\cdots-(H\,\mu_m(n-1)\frac{S(n-1)^2}{(S(n-1)+Ks\,B^d)(S(n-1)+Ks\,B^e)}X(n-1)$$
$$+I\,X(n-1))]\Big\} \tag{12}$$

Eqs. (10)–(12) can be written as shown in Eq. (13). Eq. (13) represents a system of three equations and one unknown in the form $P\mu_m(n)=l$.

$$\underbrace{\begin{bmatrix}\frac{A}{S(n)+Ks\,B^a}\\ \frac{1}{S(n)+Ks\,B^b}\\ \frac{G}{S(n)+Ks\,B^c}+\frac{H}{T_0}\frac{S(n)}{(S(n)+Ks\,B^d)(S(n)+Ks\,B^e)}\end{bmatrix}}_{P=\begin{bmatrix}P1\\P2\\P3\end{bmatrix}}\mu_m(n)$$

$$=\underbrace{\frac{1}{S(n)X(n)}\begin{bmatrix}\frac{Xd(n)-X(n-1)}{T_0}+\beta X(n)^2\\ EX(n)^2-FY_{X/S}-Y_{X/S}\frac{Sd(n)-S(n-1)}{T_0}\\ \frac{CO_2d(n)-CO_2(n-1)}{T_0}-\frac{I}{T_0}(X(n)-X(n-1))+\cdots\\ \cdots+\frac{H}{T_0}\frac{\mu_m(n-1)S(n-1)^2X(n-1)}{(S(n-1)+Ks\,B^d)(S(n-1)+Ks\,B^e)}\end{bmatrix}}_{l=\begin{bmatrix}l1\\l2\\l3\end{bmatrix}} \tag{13}$$

In order that the system can follow the reference trajectories, the system (13) must have an exact solution (see Appendix B). The coefficients matrix **P** and the independent term **l** are function of $S(n)$, therefore for the system has exact solution, the value of $S(n)$ should be such that Eq. (14) is fulfilled. The value of $S(n)$ that fulfills Eq. (14) will be named $Sez(n)$. The X, CO_2 and S errors were defined as $eX(n)=X\mathrm{ref}(n)-X(n)$, $eCO_2(n)=CO_2\mathrm{ref}(n)-CO_2(n)$ and $eS(n)=Sez(n)-S(n)$. So that the error tends to zero, it can be defined (see Appendix B):

$$\begin{aligned}&Xd(n)=X\mathrm{ref}(n)-kX[X\mathrm{ref}(n-1)-X(n-1)]\\&Sd(n)=Sez(n)-kS[Sez(n-1)-S(n-1)]\\&CO_2d(n)=CO_2ref(n)-kCO_2[CO_2ref(n-1)-CO_2(n-1)]\\&0<kX,kS,kCO_2<1\end{aligned}$$

where the rate of convergence to zero for tracking errors is function of kX, kS and kCO_2 values.

Remark 2. As can be seen an action proportional (kS, kX, kCO_2) to the error is considered.

The value of $S(n)$ makes the system in Eq. (13) has exact solution to be called $Sez(n)$, and it must be met,

$$\frac{P1}{P3}=\frac{l1}{l3}\rightarrow$$
$$\frac{\frac{A}{Sez(n)+Ks\,B^a}}{\frac{G}{Sez(n)+Ks\,B^c}+\frac{H}{T_0}\frac{Sez(n)}{(Sez(n)+Ks\,B^d)(Sez(n)+Ks\,B^e)}}=\cdots$$
$$\cdots\frac{\frac{Xd(n+1)-X(n)}{T_0}+\beta X(n)^2}{\frac{COd_2(n+1)-CO_2(n)}{T_0}-\frac{I}{T_0}(X(n)-X(n-1))+\frac{H}{T_0}\frac{\mu_m(n-1)S(n-1)^2X(n-1)}{(S(n-1)+Ks\,B^d)(S(n-1)+Ks\,B^e)}}$$

$$\frac{P1}{P2}=\frac{l1}{l2}\rightarrow$$
$$\frac{\frac{A}{Sez(n)+Ks\,B^a}}{\frac{1}{Sez(n)+Ks\,B^b}}=\frac{\frac{Xd(n)-X(n-1)}{T_0}+\beta X(n)^2}{EX(n)^2-FY_{X/S}-Y_{X/S}\frac{Sez(n)-kS[Sez(n-1)-S(n-1)]-S(n-1)}{T_0}} \tag{14}$$

Replacing $S(n)$ by Sez in the matrix **P** (Eq. (13)), and solving the three-equations system with a single unknown $\mathbf{P}\mu_m=\mathbf{l}$, whose optimal solution, by means of the minimum-squares′ method, is (Strang, 1980),

$$P^TP\mu_m=P^Tl \tag{15}$$

$$\mu_m(n)=\frac{1}{S(n)X(n)}\frac{P1l1+P2l2+P3l3}{P1^2+P2^2+P3^2} \tag{16}$$

The control action given by Eq. (16) made the tracking error tends to zero, as it is demonstrated in Appendix B.

Remark 3. To clarify the concept three equations-one-unknown and its solution see Appendix C.

3.2. Cellular death

In the cellular dead stage, the term $e^{-(CO_2-CO_{2,\,95})}/(e^{(CO_2-CO_{2,\,95})}+e^{-(CO_2-CO_{2,\,95})})$ is approximately zero, then, the evolution of the concentration of cells at this stage is determined by, From Eq. (2),

$$X_{n+1}=X_n+T_0\left(C_n\,X_n\frac{dS}{dt}\Big|_{t=nT_0}-D(T)\,X_n\right) \tag{17}$$

The parameter that depends on temperature and, that allows modifying the evolution in the cell population is $D(T)$, then, from Eqs. (11), (12) and (17),

$$D(n)=\left\{-\frac{Xd_{n+1}-X_n}{T_0}+CX_n\frac{dS}{dt}\Big|_{t=nT_0}\right\}/X_n \tag{18}$$

$$\begin{bmatrix}\frac{1}{S(n)+Ks\,B^b}\\ \frac{G}{S(n)+Ks\,B^c}+\frac{H}{T_0}\frac{S(n)}{(S(n)+Ks\,B^d)(S(n)+Ks\,B^e)}\end{bmatrix}$$
$$u_m(n)=\begin{bmatrix}EX(n)^2-FY_{X/S}-Y_{X/S}\frac{Sd(n)-S(n-1)}{T_0}\\ \frac{CO_2d(n)-CO_2(n-1)}{T_0}-\frac{I}{T_0}(X(n)-X(n-1))+\cdots\\ \cdots+\frac{H}{T_0}\frac{\mu_m(n-1)S(n-1)^2X(n-1)}{(S(n-1)+Ks\,B^d)(S(n-1)+Ks\,B^e)}\end{bmatrix} \tag{19}$$

u_m and D can be obtained by proceeding similarly than for the cellular growth phase; then, from Eqs. (6) and (7) the reference temperature, so that the desired trajectories are followed by the system, is obtained. Finally, using the controller described by Ortiz et al. (2011) can follow the trajectory of temperature obtained.

4. Experimental setup

4.1. Microorganism

The strain *Saccharomyces cerevisiae* PM16-IBT, belonging to the Institute of Biotechnology (National University of San Juan) was used. This strain was maintained on YEPD-agar medium, at 4 °C.

4.2. Bioreactor

A 20 l stainless steel stirred tank bioreactor was used for the alcoholic fermentation. The bioreactor possess the equipment for air supply, stirring, pH, and temperature control (see Fig. 1).

Fig. 1. Bioreactor layout.

4.3. Fermentation

Grape must (15 l, 216 g l^{-1} sugars) of the Pedro Jimenez varietal (from San Juan, Argentine, 2012 harvest) vine, without supplementations was inoculated with 3×10^6 yeast ml^{-1} (equivalent to 0.3 g l^{-1}), and the fermentation started at 23 °C, pH=3.5, and no aeration. Periodical mixing was provided, at 3 min at 30 rpm, every 120 min. Pressure was maintained at 1 atmosphere, which is a slight overpressure. The sample time was 3 h, the volume of each sample was 5 ml.

5. Experimental results

The process variables evolution can be seen in Fig. 2. In this case, initial cells concentration was considered as an 80% of the initial one used to generate *Xref*. In Fig. 2(a), shows that, at the beginning of the evolution, there was a difference between the signal *Xref* and the cells in the bioreactor; however after a short time interval, the system tracked the reference trajectory. The evolution of *S* is shown in Fig. 2(b). As it can be seen, in the growth phase, *S* tended to *Sez* (see Eq. (14)), and *Sez* tended to *Sref*. In Fig. 2 (c), it can be observed that CO_2 followed the reference trajectory CO_{2ref} without undesirable oscillations. Fig. 2(d) shows the temperature profile, *Tref*, which was obtained by means of Eqs. (6) and (7), and the bioreactor temperature evolution (*T*) by using the controller described in Ortiz et al. (2011). Fig. 2(d) shows how temperature keeps between 14 and 30 °C, as well.

To test the performance of the proposed controller in front of disturbances, a fermentation stop between 5 and 25 h was considered. The initials cells were selected as the 80% of the initial cells of *Xref*. Fig. 3(a) shows how cells population was maintained constant between the 5 and 25 h. Fig. 3(b) shows the evolution of *S*, as can be seen, between 5 and 25 h; the decrease of substrate

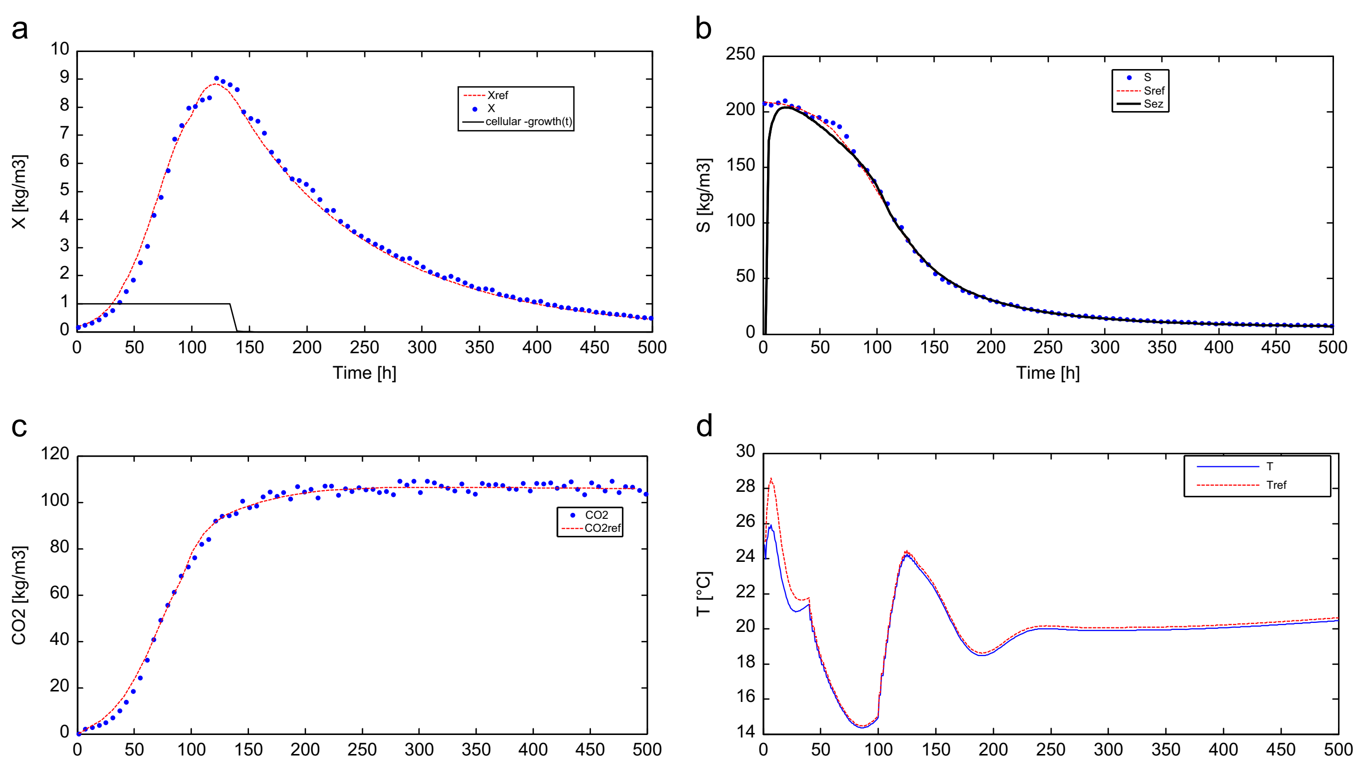

Fig. 2. (a) Time evolution of *X*. Each experimental point is the mean value of three measurements, having a mean experimental error of ±0.001 kg m^{-3}. (b) Time evolution of *S*. Each experimental point is the mean value of three measurements, having a mean experimental error of ±0.001 kg m^{-3}. (c) Time evolution of CO_2. Each experimental point is the mean value of three measurements, having a mean experimental error of ±0.1 kg m^{-3}. (d) Time evolution of *T*.

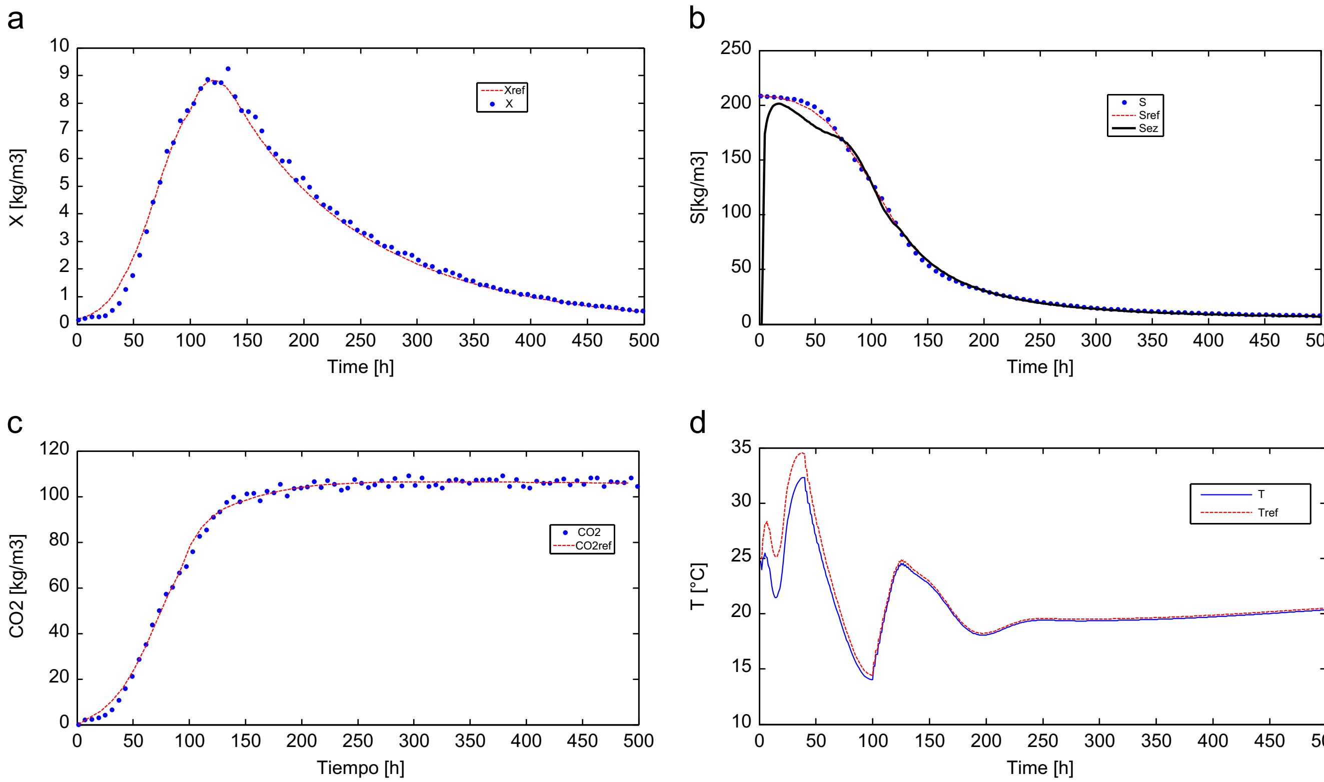

Fig. 3. (a) Time evolution of X under disturbances. Each experimental point is the mean value of three measurements, having a mean experimental error of ± 0.001 kg m^{-3}. (b) Time evolution of S under disturbances. Each experimental point is the mean value of three measurements, having a mean experimental error of ± 0.001 kg m^{-3}. (c) Time evolution of CO_2 under disturbances. Each experimental point is the mean value of three measurements, having a mean experimental error of ± 0.1 kg m^{-3}. (d) Time evolution of T under disturbances.

was lower than the reference one. This occurred because the amount of cells was lower than in an evolution corresponding to a normal fermentation. Also, it is observed that S tracks the reference trajectory.

Otherwise, it can be seen that *Sez* presented a different evolution from the observed one in Fig. 2(b). This occurred because the conditions have been changed so that the system in Eq. (12) has exact solution. Fig. 3(c) shows that the CO_2 had a very little increase during the interval where the cells were maintained constant and, then they tracked the desired trajectory. Fig. 3 (d) shows a temperature decrease that stopped the fermentation between the 5 and 25 h, and when this trouble is corrected, temperature evolved between the typical boundaries for the considered fermentation. Moreover, it can be seen that temperature never exceeds 35 °C, and is higher than 30 °C by a short time, despite the extreme disturbance at the bioreactor was submitted.

Figs. 2 and 3 show that, the control objectives have been accomplished by means of a controller that tracks very well the trajectories of the main process variables.

6. Conclusions

A new methodology based on numerical methods and linear algebra to design control algorithms for trajectory tracking in a bench-scale batch bioreactor for alcoholic fermentations to obtain good-quality varietal wines, has been presented. The proposed method allows the control of a nonlinear system, where the conditions for the tracking error tends to zero and the control actions′ calculation are obtained by analyzing a system of linear equations. This methodology is based on solving a system of linear equations at each sampling time and finding the conditions for the system of equations has solution. All experimental results have shown a good performance of the controlled system. From the achieved results, it can be concluded that the tracking error of the controller is very low for the desired trajectories corresponding to the three main process variables. In addition, including constraints on control actions and process variables will be included in a next contribution.

Acknowledgments

We gratefully acknowledge the Universidad Nacional de San Juan and the National Council of Scientific and Technological Research (CONICET), Argentina, for the financial support to carry out this work.

Appendix A

See Table A1.

Appendix B

If the bioreactor is governed by Eqs. (10)–(12) and the controller is designed by Eq. (16), then $\|e(n)\| = \|[\,eX(n) \quad eS(n) \quad eCO_2(n)\,]\| \to 0, n \to \infty$, if the *Xref*, *Sref* and $CO_{2,\ ref}$ trajectories are continuous with piecewise continuous derivatives.

$$X(n) = X(n-1) + T_0\left(A\,\mu_m(n)\frac{S(n)X(n)}{S(n)+Ks\,B^a} - \beta X(n)^2\right) \tag{A.1}$$

Defining $U(S(n))$ and applying Taylor′s series,

$$U(S(n)) = \frac{1}{S(n)+Ks\,B^a} = U(Sez(n)) + \frac{dU[S(n)+\xi(S(n)-Sez(n))]}{dS(n)}(S(n)-Sez(n)); \quad 0<\xi<1 \tag{A.2}$$

Table A1
Coefficients and parameters values in the non-isothermal model (Scaglia, Quintero, Mut, & di Sciascio, 2009b, Aballay et al., 2010).

Description		Unit	Value
Fitting coefficient			
a	–	–	1.319
b	–	–	1.282
c	–	–	1.276
d	–	–	1.152
e	–	–	1.355
A	–	–	3.119
B	Coefficient related to ethanol-tolerance	–	93.02
C	Volume of fermenting mass per substrate mass	$m^3\ kg^{-1}$	0.001
E	Volume of fermenting mass per formed cells and time	$m^3\ kg^{-1}\ h^{-1}$	1.65×10^{-4}
F	Specific rate of substrate consumption-on for cellular maintenance	$kg\ kg^{-1}\ h^{-1}$	0.01
G	CO_2 released per formed cells	$kg\ kg^{-1}$	8.073
H	CO_2 released multiplied by time per formed cells	$kg\ h\ kg^{-1}$	880.7
I	Similar to G	$kg\ kg^{-1}$	1.8
Kinetic, yield and physical-chemical parameters			
Ks	Saturation coefficient in Monod's equation	$kg\ m^{-3}$	2.15
β	Coefficient in Verlhurst's equation	$m^3\ kg^{-1}\ h^{-1}$	3.65×10^{-3}
$Y_{X/S}$	Formed cells per consumed substrate	$kg\ kg^{-1}$	0.061
$Y_{CO_2/P}$	Carbon dioxide yield coefficient based on ethanol	$kg\ kg^{-1}$	0.775
γ	Maximum cellular growth rate per Kelvin degree	$h^{-1}\ K^{-1}$	1.66
ΔG_d	Gibbs free energy change of the fermentation reaction	$kJ\ kmol^{-1}$	1916.9
E_a	Activation energy for cell growth	$kJ\ kmol^{-1}$	1928.37
E_d	Activation energy for cell death	$kJ\ kmol^{-1}$	1.7×10^5
$CO_{2\ (95)}$	CO_2 released between 85% and 95% of the maximum CO_2 released	$kg\ m^{-3}$	97.5
R	General gases constant	$kJ\ kmol^{-1}\ K^{-1}$	8.309
Do	Specific cellular death constant when temperature is 303 K	h^{-1}	0.0081
f	Coefficient that determines the increase of D_0 per degree Kelvin above 303 K	h K	3000
ρ_r	Average density of the fermenting mass	$kg\ m^{-3}$	998.204
C_{pr}	Specific heat of the fermenting mass	$W\ h\ kg^{-1}\ K^{-1}$	1.01684
V_r	Volume of the fermenting mass	m^3	0.015
Y_{H/CO_2}	Energy due to the carbon dioxide released by the bio-reaction	W h produced/kg of CO_2 released	310.3748

Then,

$$U(S(n)) = \frac{1}{S(n)+Ks\ B^a} = \frac{1}{Sez(n)+Ks\ B^a} + \frac{1}{((S(n)+\xi(S(n)-Sez(n)))+Ks\ B^a)^2}(Sez(n)-S(n)) \tag{A.3}$$

$$A\ \mu_m(n)\frac{S(n)X(n)}{S(n)+Ks\ B^a} = \underbrace{\left(\frac{AS(n)X(n)}{Sez(n)+Ks\ B^a} + \frac{AS(n)X(n)(Sez(n)-S(n))}{([S(n)+\xi(S(n)-Sez(n))]+Ks\ B^a)^2}\right)}_{S(n)X(n)U(S(n))} u_m(n) \tag{A.4}$$

Operating,

$$\frac{AS(n)X(n)}{Sez(n)+Ks\ B^a}u_m(n) = \frac{P1l1+P2l2+P3l3}{P1^2+P2^2+P3^2}\frac{A}{Sez(n)+Ks\ B^a} \tag{A.5}$$

From Eq. (14),

$$l2 = l1\frac{P2}{P1}$$

$$l3 = l1\frac{P3}{P1} \tag{A.6}$$

Replacing Eq. (A.6) in Eq. (A.5),

$$\frac{P1l1+P2^2\frac{l1}{P1}+P3^2\frac{l1}{P1}}{P1^2+P2^2+P3^2}\underbrace{\frac{A}{Sez(n)+Ks\ B^a}}_{P1} = \underbrace{\frac{Xd(n)-X(n)}{T_0}+\beta X(n)^2}_{l1} \tag{A.7}$$

Then, replacing Eq. (A.7) in Eq. (A.1),

$$X(n) = Xd(n) + T_0\frac{AS(n)X(n)(Sez(n)-S(n))}{((S(n)+\xi(S(n)-Sez(n)))+Ks\ B^a)^2}\mu_m(n) \tag{A.8}$$

If $Xd(n) = Xref(n) - kX(Xref(n-1)-X(n-1))$ is defined, then Eq. (A.8) may be expressed as,

$$\underbrace{Xref(n)-X(n)}_{eX(n)} = kx\underbrace{(Xref(n-1)-X(n-1))}_{eX(n-1)} - \cdots$$

$$\cdots - T_0\frac{AS(n)X(n)(Sez(n)-S(n))}{((S(n)+\xi(S(n)-Sez(n)))+Ks\ B^a)^2}\mu_m(n) \tag{A.9}$$

Operating in the same form with CO_2 and S,

$$\underbrace{CO_2ref(n)-CO_2(n)}_{eCO_2(n)} = kCO_2\underbrace{(CO_2ref(n-1)-CO_2(n-1))}_{eCO_2(n-1)} - \cdots$$

$$\cdots - T_0\frac{dV[S(n)+\theta(S(n)-Sez(n))]}{dS(n)}(S(n)-Sez(n))\ \mu_m(n);\ 0<\theta<1 \tag{A.10}$$

where,

$$V(S(n)) = \frac{G}{S(n)+Ks\ B^c} + \frac{H}{T_0}\frac{S(n)}{(S(n)+Ks\ B^d)(S(n)+Ks\ B^e)}$$

$$\frac{dV[S(n)+\theta(S(n)-Sez(n))]}{dS(n)} = \left.\frac{dV}{dS(n)}\right|_{S(n)+\theta(S(n)-Sez(n))} \tag{A.11}$$

$$\underbrace{Sez(n)-S(n)}_{eS(n)} = \frac{kS}{1+\frac{Y_{X/S}}{T_0((S(n)+\psi(S(n)-Sez(n)))+Ks\ B^b)^2}}\underbrace{(Sez(n-1)-S(n-1))}_{eS(n-1)}$$

$$\text{If } 0<kS<1 \Rightarrow 0 < \frac{kS}{1+\frac{Y_{X/S}}{T_0((S(n)+\psi(S(n)-Sez))+Ks\ B^b)^2}} < 1 \tag{A.12}$$

From Eq. (A.12) it can be seen, $\lim_{n\to\infty} eS(n) = 0$.
From Eqs. (A.9)–(A.11),

$$\begin{bmatrix} eX(n) \\ eS(n) \\ eCO_2(n) \end{bmatrix} = \begin{bmatrix} kX & 0 & 0 \\ 0 & kS & 0 \\ 0 & 0 & kCO_2 \end{bmatrix}\begin{bmatrix} eX(n-1) \\ eS(n-1) \\ eCO_2(n-1) \end{bmatrix} + \cdots$$

$$\cdots - T_0 \underbrace{\begin{bmatrix} \frac{AS(n)X(n)}{((S(n)+\xi(S(n)-Sez(n)))+Ks\ B^a)^2} \\ 0 \\ \frac{dV[S(n)+\theta(S(n)-Sez(n))]}{dS(n)} \end{bmatrix} \mu_m(n) eS(n)}_{Non\ \ Linearity} \tag{A.13}$$

From Eqs. (A.12) and (A.13)) and , it can be seen that, the system may be represented as a linear system plus a nonlinearity which, tends to zero.

Characterization of the nonlinearity

$$\frac{dV}{dS(n)} = -\frac{G}{(S(n)+KsB^c)^2} + \frac{H}{T_0}\frac{(S(n)+KsB^d)(S(n)+KsB^e) - S(n)(2S(n)+KsB^e+KsB^d)}{(S(n)+KsB^d)^2(S(n)+KsB^e)^2} \tag{A.14}$$

From Eq. (16),

$$\begin{aligned} \mu_m(n) &= \tfrac{1}{S(n)X(n)}\tfrac{P1l1+P2l2+P3l3}{P1^2+P2^2+P3^2} \\ l1 &= \tfrac{Xref(n)-kX(Xref(n-1)-X(n-1))-X(n-1)}{To} + \beta X(n)^2 \end{aligned} \tag{A.15}$$

Moreover, the reference trajectory fulfills,

$$Xref(n) = Xref(n-1) + \int_{(n-1)T_0}^{nT_0}\left(A\,\mu_m ref\frac{SrefXref}{Sref+Ks\ B^a} - \beta Xref^2\right)dt \tag{A.16}$$

where, $\mu_m ref$ is the value of μ_m in the reference trajectory.

From Eqs. (A.15) and (A.16)

$$\begin{aligned} l1 &= \frac{(1-kX)}{T_0}\underbrace{(Xref(n-1)-X(n-1))}_{eX(n-1)} \\ &+ \frac{1}{T_0}\int_{(n-1)T_0}^{nT_0}\underbrace{\left(A\,\mu_m ref\frac{SrefXref}{Sref+Ks\ B^a} - \beta Xref^2\right)}_{\frac{dXref}{dt}}dt + \beta X(n)^2 \end{aligned} \tag{A.17}$$

From Eq. (A.17) it can be seen that $l1$ can be expressed as a term multiplied by $eX(n)$ plus a bounded nonlinear term. Similarly, it can been proved that,

$$\begin{aligned} l2 &= \frac{-Y_{X/S}(1-kS)}{T_0}\underbrace{(Sez(n-1)-S(n-1))}_{eS(n-1)} - \frac{Y_{X/S}}{T_0}\int_{(n-1)T_0}^{nT_0}\frac{dSez}{dt}dt \\ &+ EX(n)^2 - FY_{X/S} \end{aligned} \tag{A.18}$$

$$\begin{aligned} l3 &= \tfrac{(1-kCO_2)}{T_0}\underbrace{(CO_2ref(n-1)-CO_2(n-1))}_{eCO_2(n-1)} + \tfrac{1}{T_0}\int_{(n-1)T_0}^{nT_0}\tfrac{dCO_2ref}{dt}dt \\ &- \frac{I}{T_0}(X_n - X_{n-1}) + \cdots\cdots + \frac{H}{T_0}\frac{\mu_m(n-1)S(n-1)^2X(n-1)}{(S(n-1)+Ks\ B^d)(S(n-1)+Ks\ B^e)} \end{aligned} \tag{A.19}$$

If Eqs. (A.17)–(A.19) are replaced in Eq. (16),

$$\begin{aligned} \mu_m(n) &= \tfrac{1}{S(n)X(n)(P1^2+P2^2+P3^2)} * \cdots \\ &\cdots * \left(P1\frac{1-kX}{T_0}eX(n-1) + P1\left(\frac{1}{T_0}\int_{(n-1)T_0}^{nT_0}\frac{dXref}{dt}dt + \beta X(n)^2\right)\right. \\ &- \frac{P2Y_{X/S}(1-kS)}{T_0}eS(n-1) + \cdots \\ &\cdots + P2\left(-\frac{Y_{X/S}}{T_0}\int_{(n-1)T_0}^{nT_0}\frac{dSez}{dt}dt + EX(n)^2 - FY_{X/S}\right) \\ &+ P3\frac{(1-kCO_2)}{T_0}eCO_2(n-1) + \cdots \\ &\cdots + P3\left(\frac{1}{To}\int_{(n-1)T_0}^{nT_0}\frac{dCO_2ref}{dt}dt - \frac{I}{T_0}(X_n - X_{n-1})\right. \\ &\left.\left. + \frac{H}{T_0}\frac{\mu_m(n-1)S(n-1)^2X(n-1)}{(S(n-1)+Ks\ B^d)(S(n-1)+Ks\ B^e)}\right)\right) \end{aligned} \tag{A.20}$$

If Eqs. (A.13) and (A.20) are considered,

$$v(n) = \mathbf{A}v(n-1) + \mathbf{B}(n)v(n-1) + \mathbf{Q}(n) \tag{A.21}$$

where,

$$v(n) = \begin{bmatrix} eX(n) \\ eS(n) \\ eCO_2(n) \end{bmatrix}; \quad \mathbf{A} = \begin{bmatrix} kX & 0 & 0 \\ 0 & kS & 0 \\ 0 & 0 & kCO_2 \end{bmatrix} \tag{A.22}$$

From Eqs. (A.21) and (A.22):

$$\begin{aligned} \mathbf{B}(n) &= -T_0\begin{bmatrix} \frac{AS(n)X(n)}{((S(n)+\xi(S(n)-Sez(n)))+Ks\ B^a)^2} \\ 0 \\ \frac{dVS(n)+\theta(S(n)-Sez(n))]}{dS(n)} \end{bmatrix} eS(n) * \cdots \\ &\cdots * \frac{1}{S(n)X(n)(P1^2+P2^2+P3^2)} * \left[P1\tfrac{1-kX}{T_0} \quad -\tfrac{P2Y_{X/S}(1-kS)}{T_0} \quad P3\tfrac{(1-kCO_2)}{T_0}\right] \end{aligned} \tag{A.23}$$

$$\begin{aligned} \mathbf{Q}(n) &= -T_0\begin{bmatrix} \frac{AS(n)X(n)}{((S(n)+\xi(S(n)-Sez(n)))+Ks\ B^a)^2} \\ 0 \\ \frac{dV[S(n)+\theta(S(n)-Sez(n))]}{dS(n)} \end{bmatrix} \frac{eS(n)}{S(n)X(n)(P1^2+P2^2+P3^2)} * \cdots \\ &\cdots * \left\{P1\left(\frac{1}{T_0}\int_{(n-1)T_0}^{nT_0}\frac{dXref}{dt}dt + \beta X(n)^2\right)\right. \\ &+ P2\left(-\frac{Y_{X/S}}{T_0}\int_{(n-1)T_0}^{nT_0}\frac{dSez}{dt}dt + EX(n)^2 - FY_{X/S}\right) + \cdots \\ &\cdots + P3\left(\frac{1}{To}\int_{(n-1)T_0}^{nT_0}\frac{dCO_2ref}{dt}dt - \frac{I}{T_0}(X_n - X_{n-1})\right. \\ &\left.\left. + \frac{H}{T_0}\frac{\mu_m(n-1)S(n-1)^2X(n-1)}{(S(n-1)+Ks\ B^d)(S(n-1)+Ks\ B^e)}\right)\right\} \end{aligned} \tag{A.24}$$

where, $\mathbf{B}_n$ and $\mathbf{Q}_n$ are bounded, and moreover it is true that $\mathbf{B}_n, \mathbf{Q}_n \to 0 n \to \infty$, due to the $\lim_{n\to\infty} eS(n) = 0$.

$$v_n = \mathbf{A}^n v_0 + \sum_{l=1}^{n}\mathbf{A}^{n-l}[\mathbf{B}_l v_{l-1} + \mathbf{Q}_l] \tag{A.25}$$

$$v_n = \mathbf{A}^n v_0 + \sum_{l=1}^{n}\mathbf{A}^{n-l}\mathbf{B}_l v_{l-1} + \sum_{l=1}^{n}\mathbf{A}^{n-l}\mathbf{Q}_l \tag{A.26}$$

$$\|v_n\| \le \|\mathbf{A}^n v_0 + \sum_{l=1}^{n}\mathbf{A}^{n-l}\mathbf{B}_l v_{l-1}\| + \|\sum_{l=1}^{n}\mathbf{A}^{n-l}\mathbf{Q}_l\| \tag{A.27}$$

$$\|v_n\| \le c0[\delta(1+c2)]^{n-k1} + \|\sum_{l=1}^{n}\mathbf{A}^{n-l}\mathbf{Q}_l\| \tag{A.28}$$

$$\|\sum_{l=1}^{n}\mathbf{A}^{n-l}\mathbf{Q}_l\| \le \max\sqrt{({\mathbf{Q}_{1n}}^2 + {\mathbf{Q}_{2n}}^2)}|eS(0)|\|\sum_{l=1}^{n}\mathbf{A}^{n-l}kS^l\| \tag{A.29}$$

where $eS(0)$ is the initial substrate error and $0 < kS < 1$.

It always can be chosen $\delta(1+c2) < 1$, (Agarwal, 2000 (Theorem 5.2.3, pp. 240–241)), applying Toeplitz Lemma, (Agarwal, 2000 (pp. 682)), it is true that,

$$\lim_{n\to\infty}\sum_{l=1}^{n}\mathbf{A}^{n-l}k\theta^{l-1} = 0 \tag{A.30}$$

Then, from Eqs. (A.28)–(A.30),

$$\lim_{n\to\infty}\|v_n\| = 0$$

Appendix C

This section will be discussed, using a numerical example, the concept of multiple equations one-unknown. In this paper this concept is used to find the control actions so that the tracking errors tend to zero. The value of one of the parameters (S) of the system (13) is determined on each sampling period, so that (13) has exact solution (the value that fulfills this is called S_{ez}). Then, is possible determining the value of the control action (so that the tracking errors tend to zero) solving the system (13).

Using a numerical example the three equations and one-unknown concept is show; the objective is to find the condition (S_{ez}) for which the system (A.31) has exact solution, after that the system of linear equations is solved to determine the value of the unknown x.

Given the system defined by Eq. (A.31),

$$\underbrace{\begin{pmatrix} S^2-10S+10 \\ S^2-6S+8 \\ 4S \end{pmatrix}}_{a} x = \underbrace{\begin{pmatrix} 2 \\ 6 \\ 8 \end{pmatrix}}_{b} \tag{A.31}$$

In order to the system (A.31) has exact solution, the vector **a** must be parallel to **b**. Thus, (A.32) must be fulfilled:

$$a//b \Rightarrow \begin{cases} \frac{S^2-6S+8}{S^2-10s+10} = \frac{6}{2} = 3 \Rightarrow 2S^2-24S+22=0 \begin{cases} S=1 \\ S=11 \end{cases} \\ \frac{S^2-10S+10}{4S} = \frac{6}{8} = \frac{3}{4} \Rightarrow S^2-9S+8=0 \begin{cases} S=1 \\ S=8 \end{cases} \end{cases}$$

$$\Rightarrow S_{ez}=1 \tag{A.32}$$

Eq. (A.32) shows how the system (A.31) is forced to have exact solution by calculating S_{ez}. Then, replacing S by S_{ez} in (A.31) is possible to compute the value of the unknown x:

The solution given by (A.33) can be obtained by least squares,

$$\mathbf{a}^T\mathbf{a}x = \mathbf{a}^T\mathbf{b} \Rightarrow (1 \quad 3 \quad 4)\begin{pmatrix} 1 \\ 3 \\ 4 \end{pmatrix} x = (1 \quad 3 \quad 4)\begin{pmatrix} 2 \\ 6 \\ 8 \end{pmatrix}$$

$$\Rightarrow 26x = 52 \Rightarrow x = 2 \tag{A.33}$$

Through this numerical example has been shown how it is possible force to the system to has exact solution and then calculate the unknown.

References

Aballay, P. M., Scaglia, G. J. E., Vallejo, M. D. & Ortiz, O. A. (2008). Non isothermal phenomenological model of an enological fermentation: modelling and performance analysis. In: *10th International chemical and biological engineering conference CHEMPOR 2008*. Braga, Portugal. 4–6 September.

Aballay, P. M., Scaglia, G. J. E., Vallejo, M. D., Rodríguez, L. A. & Ortiz, O. A. (2010). Non-isothermal model of the yeasts growth in alcoholic fermentations for high quality wines. In: *Seventh international Mediterranean and Latin American modeling multiconference—I3M2010.* Fes, Morocco. 13–15 October.

Agarwal, R. (2000). *Difference equations and inequalities, theory, methods, and applications*. New York, N.Y.: Marcel Dekker, Inc.

Casalta, E., Aguera, E., Picou, C., Rodriguez-Bencomo, J. J., Salmon, J. M., & Sablayrolles, J. M. (2010). A comparison of laboratory and pilot-scale fermentations in winemaking conditions. *Applied Microbiology and Biotechnology*, *87*(5), 1665–1673.

Cédric, D., Michel, B., Lionel, B., Brigitte, G., & Chabriat, J. (2011). Multivariable linearizing control of an industrial sugar crystallization process. *Journal of Process Control*, *21*(2011), 46–54.

Coleman, M. C., Fish, R., & Block, D. E. (2007). Temperature-dependent kinetic model for nitrogen-limited wine fermentations. *Applied and Environmental Microbiology*, *73*(18), 5875–5884.

Colombié, S., Malherbe, S., & Sablayrolles, J. M. (2007). Modeling of heat transfer in tanks during wine-making fermentation. *Food Control*, *18*, 953–960.

Golshan, M., MacGregor, J. F., Bruwer, M., & Mhaskar, P. (2010). Latent variable model predictive control (LV-MPC) for trajectory tracking in batch processes. *Journal of Process Control*, *20*(2010), 538–550.

Henson, M. A. (2003). Dynamic modeling and control of yeast cell populations in continuous biochemical reactors. *Computers & Chemical Engineering*, *27*(8-9), 1185–1199.

Horn, J. (2001). Trajectory tracking of a batch polymerization reactor based on input–output-linearization of a neural process model. *Computers and Chemical Engineering*, *25*(2001), 1561–1567.

Komives, C., & Parker, R. (2003). Bioreactor state estimation and control. *Current Opinion in Biotechnology*, *14*, 468–474.

Li, P., & Wozny, G. (2001). Tracking the predefined optimal policies for multiple-fraction batch distillation by using adaptive control. *Computers and Chemical Engineering*, *25*(2001), 97–107.

Malherbe, S., Fromion, V., Hilgert, N., & Sablayrolles, J. M. (2004). Modeling the effects of assimilable nitrogen and temperature on fermentation kinetics in enological conditions. *Biotechnology and Bioengineering*, *86*(3), 261–272.

Molina, A. M., Swiegers, J. H., Varela, C., Pretorius, I. S., & Agosin, E. (2007). Influence of wine fermentation temperature on the synthesis of yeast-derived volatile aroma compounds. *Applied Microbiology and Biotechnology*, *77*, 675–687.

Morari, M., & Zafiriou, E. (1997). *Robust process control*. UK: Pearson Education.

Ortiz O. A., Vallejo M. D., Scaglia G. J. E., Mengual C. A. & Aballay P. M. (2009). Advanced temperature tracking control for high quality wines using a phenomenological model. In: *10th International symposium on process systems engineering—PSE2009,* Salvador Brasil, August p. 16–20, 2009.

Ortiz, O. A., Aballay, P. M. & Vallejo, M. D. (2006). Modelling of the killer yeasts growth in an enological fermentation by means of a hybrid model. In: *XXII Interamerican congress of chemical engineering and V Argentinian congress of chemical engineering. Innovation and management for sustainable development,* A. 13b-224, 451–452. Buenos Aires, Argentina. 1–4 October.

Phisalaphong, M., Srirattana, N., & Tanthapanichakoon, W. (2006). Mathematical modeling to investigate temperature effect on kinetic parameters of ethanol fermentation. *Biochemical Engineering Journal*, *28*, 36–43.

Pretorius, I. S. (2000). Tailoring wine yeast for the new millennium: novel approaches to the ancient art of winemaking. *Yeast*, *16*, 675–729, http://dx.doi.org/10.1002/1097-0061(20000615)16:8 < 675::AID-YEA585 > 3.0.CO;2-B.

Romero Cascales, I. (2008). Extracción de compuestos fenólicos de la uva al vino, Papel de las enzimas de maceración. *Tesis Doctoral (PhD Thesis), Universidad de Murcia*, Spain.

Rosales, A., Scaglia, G. J. E., Mut, V., & di Sciascio, F. (2011). Formation control and trajectory tracking of mobile robotic systems—A Linear Algebra approach. *Robotica*, *29*, 335–349, http://dx.doi.org/10.1017/S0263574710000068.

Rosales, A., Scaglia, G. J. E., Mut, V., & di Sciascio, F. (2009). Trajectory tracking of mobile robots in dynamic environments—A linear algebra approach. *Robotica*, *27*(07), 981–997.

Sablayrolles, J. M. (2009). Control of alcoholic fermentation in winemaking: Current situation and prospect. *Food Research International*, *42*, 418–424.

Scaglia, G. J., Rosales, A., Quintero, L., Mut, V., & Agarwal, R. (2010b). A linear-interpolation-based controller design for trajectory tracking of mobile robots. *Control Engineering Practice*, *18*(2010), 318–329.

Scaglia, G. J. E., Quintero, O. L., Mut, V., & di Sciascio, F. (2009b). Numerical methods based controller design for mobile robots. *Robotica*, *27*(02), 269–279 (Mar 2009).

Scaglia, G. J., Aballay, P. M., Vallejo, M. D., Suarez, G. I. & Ortiz, O. A. (2010). Numerical methods based controller design applied to a high quality wines bioprocess. VI Argentinean congress of chemical engineering: contributions from the chemical engineering developments and opportunities for the XXI Century, Single vol., 05g (1223), pp. 125–126. 26–29 September, Mar del Plata (Argentina).

Scaglia, G. J. E., Aballay, P. M., Mengual, C. A., Vallejo, M. D., & Ortiz, O. A. (2009a). Improved phenomenological model for an isothermal winemaking fermentation. *Food Control*, *20*, 887–895.

Sjoberg, J., & Agarwal, M. (2002). Trajectory tracking in batch processes using neural controllers. *Engineering Applications of Artificial Intelligence*, *15*(2002), 41–51.

Stoer, J., & Bulirsch, R. (1992). *Introduction to numerical analysis*. New York, N.Y.: Springer-Verlag.

Strang, G. (1980). *Linear algebra and its applications*. New York: Academic Press.

Tebbani, S., Dumur, D., & Hafidi, G. (2008). Open-loop optimization and trajectory tracking of a fed-batch bioreactor. *Chemical Engineering and Processing*, *47* (2008), 1933–1941.

Torija, M. J., Beltran, G., Novo, M., Poblet, M., Guillamón, J. M., Mas, A., et al. (2003). Effects of fermentation temperature and Saccharomyces species on the cell fatty acid composition and presence of volatile compounds in wine. *International Journal of Food Microbiology*, *85*, 127–136.

Valencia Peroni, C. (2003). *Optimization and control of fed-batch fermentation processes by using neural systems*. Ph. D. Thesis. Universitat Rovira I Virgili. Barcelona, Spain.

Vallejo, M. D., Aballay, P. M., Toro, M. E., Vazquez, F., Suarez, G. I. & Ortiz, O. A. (2005), Hybrid modeling and neural prediction of the wild killer yeast fermentation performance in a winemaking process. *2nd Mercosur congress on chemical engineering and fourth Mercosur congress on process systems engineering, paper code 230.* 1–10. Rio de Janeiro, Brazil. 14–18 August.

Zenteno, M. I., Pérez-Correa, J. R., Gelmi, C. A., & Agosin, E. (2010). Modeling temperature gradients in wine fermentation tanks. *Journal of Food Engineering*, *99*, 40–48.